Study of surface modification of recycled ultrafiltration membranes using statistical design of experiments

L. Rodríguez-Sáez[a,b,*], J. Landaburu-Aguirre[a], S. Molina[a], C. García-Payo[c], E. García-Calvo[a,b]

[a]*IMDEA Water Institute, Avenida Punto Com, 2, 28805. Alcalá de Henares, Madrid, Spain*

[b]*Chemical Engineering Department, University of Alcalá, Ctra. Madrid-Barcelona Km 33.600, 28871. Alcalá de Henares, Madrid, Spain*

[c]*Department of Structure of Matter, Thermal Physics and Electronics, Faculty of Physics, University Complutense of Madrid, Avda. Complutense s/n, 28040 Madrid, Spain*

Abstract

Membrane surface modification on recycled ultrafiltration membrane was conducted using statistical design of experiments by two levels full factorial design. Dip-coting using catechol (CA) and polyetylenimine (PEI) was chosen as the membrane surface modification method because its simplicity, energy saving characteristics and bio-based character. The factors studied were: CA and PEI concentration (1g/l and 4 g/l), temperature (30ºC and 50ºC) and reaction time (2 and 7 hours). The studied responses were the relative permeability (*Pr*) and the flux recovery ratio (FRR). A model with good validity was obtained for both responses. Membranes were deeply characterized using several techniques: Scanning electron microscopy (SEM); Attenuated total reflectance–Fourier transform infrared (ATR–FTIR) spectroscopy; X-ray photoelectron spectroscopy (XPS) and Atomic force microscopy (AFM). Statistical design of experiments resulted on a useful tool to understand how the factors affect the surface modification. Surface modification conducted at mild conditions (2 hours; 30 ºC and 1g/l) improved membrane permeability and flux recovery ratio. Moreover, interaction between

factors turned out to be significant in the modification process which was an unexplored field in previous works. Modification of recycled membranes is an innovative process that follows a Circular Economy approach.

Keywords: End-of-life membrane; Statistical design of experiments; Surface modification; Surface characterization; Recycling; Ultrafiltration.

** Corresponding author at: IMDEA Water Institute, Avenida Punto Com, 2, 28805. Alcalá de Henares, Madrid, Spain. Tel.: +34 918 30 59 62. E-mail addresses: laura.rodriguez@imdea.org.*

1. Introduction

Membrane technology is widely used for wastewater treatment and many other technological and environmental processes for many years now. This technology has been also deeply improved over the years [1,2]. Specifically, reverse osmosis (RO) technology is broadly implemented [3]. The most used membranes for this purpose are aromatic polyamide (PA) based membranes. The main drawbacks related to membrane performance have been identified to be the energy consumption, membrane fouling and the membrane replacement rate [4,5]. Most of the countries manage the disposal of RO membranes according to their own legislation which means that, normally, most of them end up on landfills following the traditional model of linear economy [6]. Nonetheless, this current practice goes against the European Union principles associated to Circular Economy [7,8].

Related to EoL RO membranes, several alternative scenarios to landfill disposal have been considered [9,10]. Framed on Life Cycle Assessment (LCA), Lawler *et al.* [11] studied the EoL RO membranes disposal alternatives in order to compute the environmental impact of each one. Conclusion resulting of that research showed that landfill disposal was the least environmentally friendly option. On the contrary, direct reuse turned out to be the most environmentally favorable alternative, which consists on using the membrane module without altering the structure of the module itself. Nonetheless, the condition of EoL RO membranes modules does not always allow the direct reuse. Considering this issue, RO membrane recycling is also possible by varying or eliminating their membrane active layer using an oxidant chemical such as sodium hypochlorite (NaClO). By mean of this procedure, it is possible to achieve ultrafiltration (UF) membranes by totally removing the active polyamide layer [6,12,13].

Several studies have already presented the use of recycled UF membranes for wastewater treatment processes [14–16]. Still, performance parameter, such as permeability of recycled UF membranes should be further studied along with fouling behavior, operational costs saving, energy consumption reduction, resource recovery, etc. [17–19]. Under this framework, Senán-Salinas *et al.* has recently developed a study of a comparative LCA and cost-effectiveness analysis of the recycled membranes, having into consideration as a primordial factor, among others, the permeability of the recycled membranes, which is significantly smaller compared with the commercial ones [20].

Numerous actions can be taken in order to improve the membranes performance by enhancing the permeability or minimizing the membrane fouling such as: i) to experience different operational strategies [21–23]; ii) to create novel material membranes [24] or iii) to modify/functionalize membranes [25–27]. Membrane surface modification has been deeply studied during the last years and numerous techniques and procedures have been tested for this purpose [28–31]. Several studies like the one developed by Nady *et al*. [32] or Ayyavoo *et al.* [33] highlighted coating process because its i) simplicity; ii) reproducibility; iii) environmentally friendly behavior and iv) cost effectiveness. Regarding the use of compounds and/or particles for the membrane surface modification, main actions to this matter have been focused on the use of several hydrophilic chemical compounds that are attached to the membrane, avoiding the adsorption of the fouling agents related to biofouling. Some of these methods use very well-known chemical compounds such as i) polyethylene glycols (PEG´s) [26]; ii) nanoparticles [34]; iii) polyaniline [35]; iv) novel bio-inspired materials like polydopamine (PDA) [36,37] or v) other interesting and novel paths such as the use of enzyme catalysis, i.e. laccases, to functionalize membranes. [27].

In the present work, dip-coating process was used to modify the recycled membranes. The use of this methodology involves that permeability could be compromised [38,39]. To obtain an improvement and environmentally friendly character of the membranes, eco-friendly compounds such as catechol (CA) and polyethylenimine (PEI) were selected for current investigation.

Several previous studies using CA and PEI have been carried out. Yan Chau Xu *et al.* studied the co-deposition of CA and PEI with different molecular weights (Mw) [39]. Xue *et al.* studied a combined CA and PEI surface modification along with a surface mineralization for the membranes [40]. Qiu *et al.* employed an initial reaction time for co-deposition of CA and PEI with a constant stirring of the solution at room temperature. After that, further grafting reactions with different PEI Mw were conducted [41]. Other studies to take into consideration for the topic is the one developed by Zhang *et al.* [36] using PDA and PEI in a covalent grafting reaction.

The studies mentioned above were conducted following the traditional one factor at a time approach, where the effect of each factor is studied separately. However, this approach implies a significant number of experiments and, therefore, an inefficient use of resources. In addition, it may often miss important conclusions about the effect of (one) experimental variable when the level of another variable is changed (i.e. interaction effects) [42]. The use of statistical experimental design such as factorial designs overcome these limitations and reduces the number of experiments needed for the analysis of the main effects, decreasing the use of time, raw material, and natural resources.

The aim of the present work is to gain, by means of statistical design of experiments, a deep understanding of the main factors affecting the surface modification of recycled ultrafiltration membranes. Also, as a novelty, the interaction between factors will be

studied to understand if they have any impact in the modification reaction and, therefore, in the membrane performance. Moreover, membrane surface characterization will be conducted to contrast obtained results.

2. Experimental part

2.1. Materials

Coupons (216 cm^2 area) from recycled EoL RO membrane model TM720-400 (Toray) were used. The chemicals consumed along this study were sodium hypochlorite (NaClO 10 % w/v), ethanol (96% EPR Ph.Eur. LABKEM (Spain)), polyethylenimine, branched (average Mw 800 by LS, average MN 600 by GPG. ALDRICH), 1,2-dihydroxybenzene (ReagentPlus®, ≥99% by Sigma Aldrich), Trizma hydrochloride (reagent grade ≥ 99.0%, SIGMA (Spain)), Trizma base (reagent grade ≥ 99.9% primary standard and buffer were purchased from SIGMA (Spain)), Bovine Serum Albumine (MW: 67 kDa) (lyophilized powder, ≥96% agarose gel electrophoresis by SIGMA), E. coli (CECT434 (batch 23/03/2017)). Samples and solutions were prepared using Milli-Q water.

2.2. Membrane recycling and modification

Recycled UF membranes were obtained by removing the polyamide layer of the EoL RO membranes. For this purpose the process developed was the one described at Pacheco *et al* [6]. The recycling process was performed with a passive transformation pilot applied to the whole module, maintaining its integrity [16]. After that, a membrane autopsy was conducted. Module was opened to obtain membrane samples to characterize and to use for filtration and fouling experiments. The modification step was conducted by one step co-deposition using CA and PEI. pH adjustment was made by means of tris-buffer solution (pH).

As Figure 1 shows, membranes were attached to the modification system to remain vertically during the dip coating process. After surface modification, membranes were rinsed with Milli-Q water in order to remove any CA/PEI co-deposition particles left.

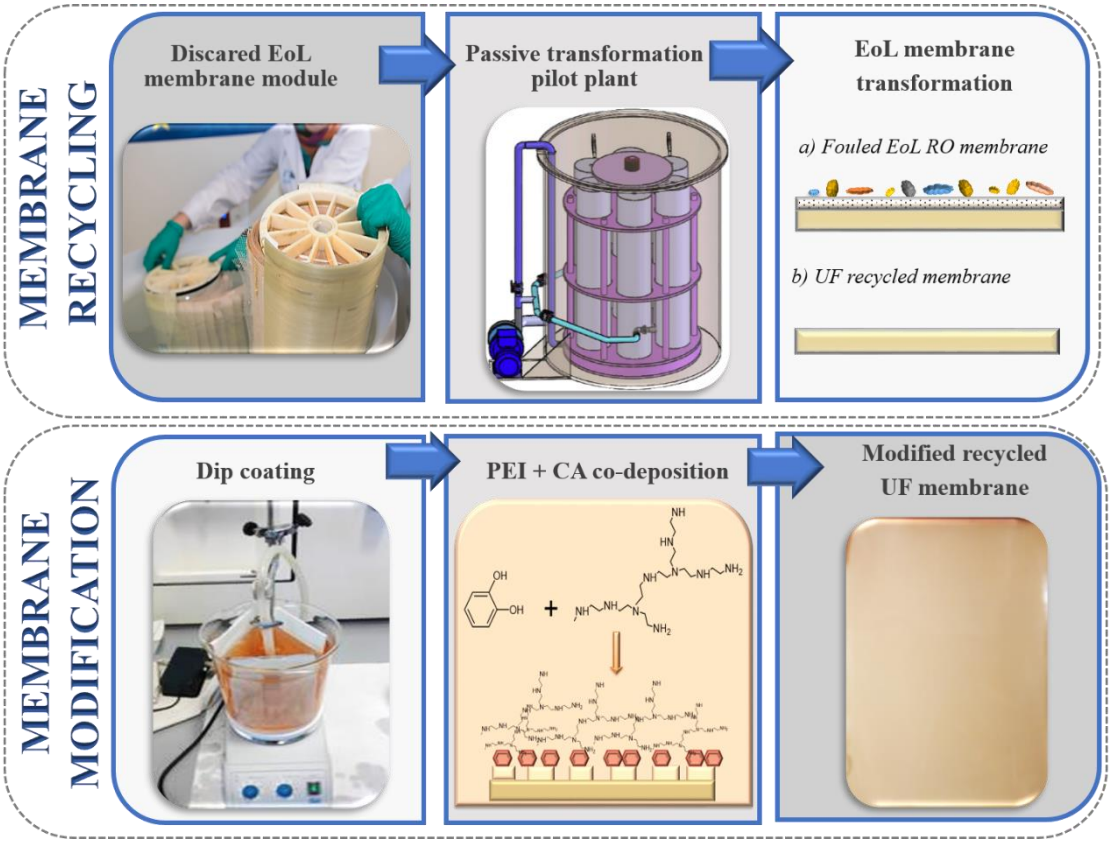

Figure 1. Membrane preparation flow chart

2.3. Statistical Design of Experiments: permeability and flux recovery ratio

MODDE Go software (Umetrics) was used for the design of experiments and data analysis. Specifically, a two-level full factorial design was employed. The factors studied were i) concentrations of CA (CCA), ii) concentration of PEI (CPEI), iii) exposure time (t) and iv) temperature (T). Three center points were added to the experimental set. The process performance of the membranes was defined in terms of two main responses i) relative permeability (Pr) and ii) flux recovery ratio (FRR). Preliminary results show that permeability values on recycled membranes varied from 0% to 35%. Due to the experimental variability of the permeability of the recycled

membrane coupons, the permeability values were normalized by calculating the relative<e permeability P_r.

The responses were obtained by conducting the filtration experiments as follows:

Filtration experiments

Filtration experiments were conducted in a stirred cell (Merk Stirred Cell XFUF04701) with an effective membrane area of 4.7 $x10^{-2}$ m^2 at room temperature. The flat sheet membranes used were i) recycled UF and ii) modified recycled UF membranes.

The *FRR* of the membranes was estimated using a solution of Bovine Serum Albumin (BSA) at 1 g/L solution concentration as fouling agent.

Each experiment was divided in the subsequent steps: i) Milli-Q water was forced to pass through the membrane at the stipulated pressure to obtain an initial permeability value, ii) BSA (1 g/L) solution pass at the specified pressure, iii) the membrane was extracted to receive a manual cleaning with Milli-Q water, iv) Milli-Q water was enforced to go through the membrane and v) lastly, a last permeability test with clean Milli-Q water was done.

Permeability (*P*; $L \cdot m^{-2} \cdot h^{-1} \cdot bar^{-1}$), was calculated as follows (equation (1)):

$$P = {J}/{TMP} \qquad (1)$$

Where *TMP* (bar) is the transmembrane pressure and *J* ($L \cdot m^{-2} \cdot h^{-1}$) is the permeate flux of the studied membranes (equation (2)):

$$J = \frac{Q}{S \times h} \qquad (2)$$

Where Q (L.h^{-1}) is the membranes permeate flow, S (m^2) represents the membrane surface and h shows time in hours.

Permeate flow (Q), at laboratory, was calculated by measuring permeate weight (W, g) according to time (t, h). Solution density (ρ, g/L) considered was 1,000 g/l (equation (3)):

$$Q = \frac{W}{\rho \times t} \quad (3)$$

Relative permeability (P_r) was obtained dividing the individual permeability (P_i) obtained for each coupon over the average permeability ($P_{average}$) of all coupons studied (equation (4)).

$$P_{r=P_i/P_{average}} \quad (4)$$

The value of *FRR* was calculated as (equation (5))

$$FRR = {J_2}/{J_1} \quad (5)$$

Where J_1 (L·m^{-2}·h^{-1}) is the Milli-Q water permeability before BSA experiment and J_2 (L·m^{-2}·h^{-1}) is the Milli-Q water permeability after BSA experiment.

Model validity

The validity of the empirical models fitted with multiple linear regressions (MLR) was tested with analysis of variance (ANOVA). The confidence level used was 95%. The

model was also evaluated in terms of the coefficient of determination (R^2), adjusted coefficient of determination (R^2_{adj}) and the response variation percentage predicted by the model according to cross validation (Q^2= 1–PRESS/SS); PRESS is the prediction residual sum of squares and SS is the total sum of squares of Y corrected for the mean). Table 1 shows all the experiment conducted for fitting the model. As Table 1 shows, three center points were included to analyze the reproducibility of the experiments.

Table I Conducted experiments.

Factorial Design				
Membrane	**CCA (g/l)**	**CPEI (g/l)**	**T (ºC)**	**t (hours)**
1	1	1	30	2
2	4	1	30	2
3	1	4	30	2
4	4	4	30	2
5	1	1	50	2
6	4	1	50	2
7	1	4	50	2
8	4	4	50	2
9	1	1	30	7
10	4	1	30	7
11	1	4	30	7
12	4	4	30	7
13	1	1	50	7
14	4	1	50	7
15	1	4	50	7
16	4	4	50	7
17	2.5	2.5	40	4.5
18	2.5	2.5	40	4.5
19	2.5	2.5	40	4.5

Given the results of the fitted model, four membranes were selected for surface characterization. To obtain a fine representation of parameters' level, the selected membranes were *nº 1, nº 5, nº 9* and *nº 13*. Moreover, a *blank* membrane (recycled membrane with no modification conducted) was also characterized.

2.4. Membrane surface characterization

To assess if the modification was successful and to determinate its intensity, membrane surface characterization was conducted. Scanning electron microscopy (SEM) employing S-8000 Model (Hitachi) image device was employed to examine the surface

of the membranes. Furthermore, to determine the average pore diameter of modified membranes, Digital Image Analysis (DIA) was performed by using ImageJ software (Java-based image processing program) for porous size analysis [43]. Attenuated total reflectance–Fourier transform infrared (ATR–FTIR) spectroscopy using a Perkin-Elmer RX1 spectrometer was used to analyze the functional group on the membrane surface. To investigate the surface chemical composition of the membranes, X-ray photoelectron spectroscopy (XPS) was conducted with a SPECS system (Berlin, Germany) equipped with Phoibos 150 1D-DLD analyzer and monochromatic radiation source Al Kα (1486.7 eV) (wide scan: step energy 1 eV, dwell time 0.1 s, pass energy 80 eV). Specific analysis of the detected elements was performed (detail scan: step energy 0.08 eV, dwell time 0.1 s, pass energy 30 eV) with an exit angle of the electrons of 90º. The roughness of the membrane surfaces was examined by atomic force microscopy (AFM) using a Multimode topographical AFM (Vecco Instruments, Santa Barbara, California) equipped with a Nanoscope Iva control system (software version 6.14r1). Silicon tapping probes (RTESP, Veeco) were used with a resonance frequency of ~300 kHz and a scan rate of 0.5 Hz, 5 × 5, 3 × 3, 2 × 2 y 1 × 1 μm2 AFM images were taken for each sample.

3. Results

3.1. Model validity

When evaluating the validity of the fitted model for the relative permeability with ANOVA results (Table 2), it shows that F_{value} (10.893) > $F_{tabulated}$ (3.135) and $p < 0.05$. Therefore, the regression model is statistically significant with the 95% confidence level. In addition, the lack of fit is not significant with the 95% confidence level ($p > 0.05$). The coefficient of determination, R^2 (0.884), and the response variation

percentage predicted by the model, Q^2 (0.674), also show a good validity of the model developed.

Table II ANOVA table for relative permeability model.

P_r	DF	SS	MS	F_{value}	$F_{tabulated}$ (α=0,05)	Probability (p)	SD
Total	18	15.5592	0.8644				
Constant	1	15.272	15.272				
Total corrected	17	0.287178	0.0168928				0.129972
Regression	7	0.253883	0.036269	10.8932	3.315	0.001	0.190444
Residual	10	0.033295	0.0033295				0.0577018
Lack of Fit	8	0.0328284	0.00410354	17.5867	19.371	0.055	0.0640589
Pure error	2	0.00046667	0.00023333				0.0152752

When evaluating the validity of the fitted model for the FRR with ANOVA results (Table 3), it shows that F_{value} (7.053) > $F_{tabulated}$ (4.0600) and $p < 0.05$. Therefore, the regression model is statistically significant with the 95% confidence level. In addition, the lack of fit is not significant with the 95% confidence level ($p > 0.05$). The coefficient of determination, R^2 (0.746), and the response variation percentage predicted by the model, Q^2 (0.529) also show an acceptable validity of the model developed.

Table III ANOVA table for FRR model.

FRR	DF	SS	MS	F_{value}	$F_{tabulated}$ (α=0,05)	Probability (p)	SD
Total	18	19.6349	1.09083				
Constant	1	17.9401	17.9401				
Total corrected	17	1.69485	0.099697				0.315748
Regression	5	1.26443	0.252886	7.05036	3.11	0.003	0.502877
Residual	12	0.430421	0.0358685				0.18939
Lack of Fit	10	0.396555	0.0396555	2.34186	19.40	0.336	0.199137
Pure error	2	0.0338667	0.0169333				0.130128

3.2. Effects of factors and its interactions on permeability

Based on the satisfactory model obtained, the effect of factors and interaction between factors on the permeability could be evaluated (Figure 2). CCA has not been taken into

consideration for the analysis since, according to the model, it has no significant effect. This might be due to the range of CCA used in the present study. As Figure 2 illustrates, the principal factor affecting permeability values is CPEI, having a negative effect on it. This means that when CPEI increases, permeability decreases. This might be because, at higher PEI concentration, more PEI molecules are attached to the membrane surface, obtaining a thicker modification layer that adds a higher resistance to the water flow, reducing the permeability [36,39,44].

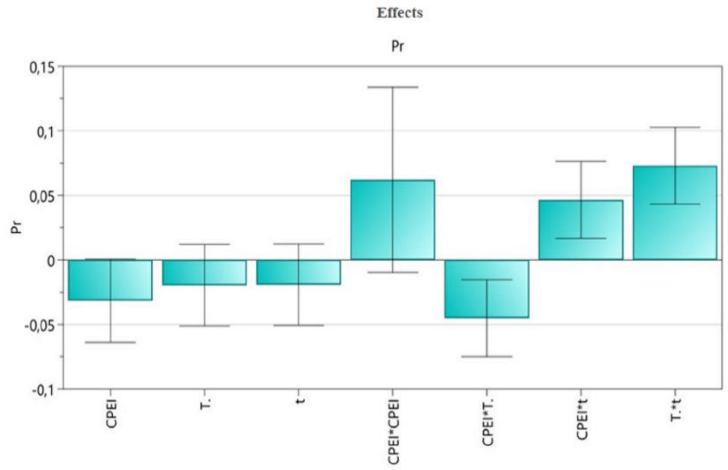

Figure 2 Effects on relative permeability (MODDE_12 Software). 95% confident level is shown as error bar.

It is important to note that also three main interactions seem to be statistically significant (Figure 3). When an interaction between two factors is significant, the effect of one of the factors depends on the level of the other factor, i.e. the factors are not independent from each other. There is evidence that previous studies did not take into consideration the importance of the interaction between factors and this could mean obtaining incomplete conclusions. For instance, Xu *et al.* conducted the experiments with same reaction time (6 hours), temperature (30ºC) and chemical compounds ratio (1:1; 3g/L) modifying, only PEI Mw. Xu *et al* concluded that low Mw of PEI provided a thinner coating layer along with an excellent separation characteristic, especially with PEI Mw 600. However, the levels of the remaining factors present on the experiments

had not been evaluated and, consequently, it is difficult to evaluate if at high temperature levels or lower reaction times the results would be similar [39]. Xue *et al.* carried out the experiments with variations of CA/PEI mass ratio (1.2 g/L of CA) and co-deposition time but same temperature (25 ºC) preparing the membrane for an additional modification. Xue *et al.* concluded that the most suitable reaction conditions were CA concentration 1.2 g/l, mass ratio CA: PEI 4:1 and 8 hours reaction time, respectively. Once more, it is not possible to infer what the results would have been with temperature variation [40]. Zhang *et al*. developed a surface modification using PEI and PDA and they took into consideration the variation of some of the parameters involved in the reaction (PEI concentration, temperature or reaction time). Even though Zhang *et al*, did not study the effect of interactions between factors, they discussed the possible effects that PEI concentration, temperature and time could have into the chemical reaction. The study of Zhang *et al.* concluded that mild modified membranes showed quite good performance and that controlling modification parameters, different modification layers and membrane performance can be achieved [36].

As Figure 3 shows, in this study three main interactions seem to be statistically significant: i) CPEI-temperature; ii) CPEI-time and iii) temperature-time (Figure 3).

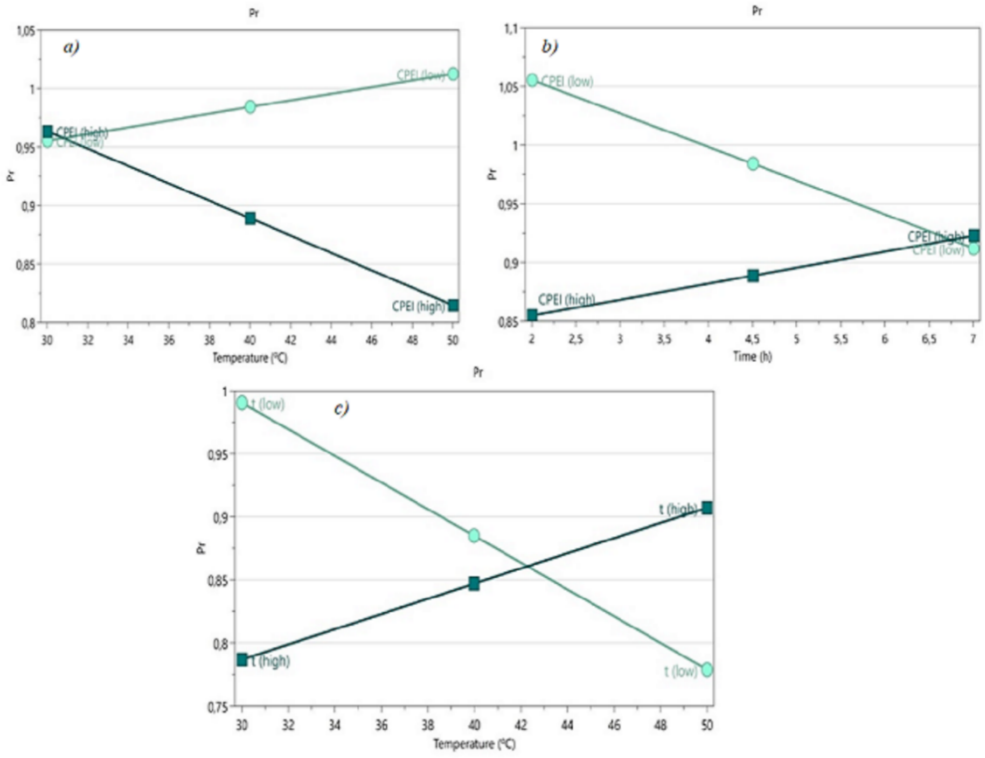

Figure 3. Interactions affecting relative permeability: a) CPEI - Temperature; b) CPEI – Time; c) Temperature – Time

i) CPEI - Temperature (Figure 3a): The effect of CPEI has not a significant effect when temperature is low. Nevertheless, when membrane modification was made at higher temperature the high values of CPEI have a clear negative effect on permeability. As Zhang *et al.* had already observed, this may be due to Schiff base reaction or/and Michael addition, which are both endothermic reactions. This could mean that the temperature allows more molecules to attach to the membrane surface. Then, the thickness could be higher along with temperature affecting, consequently, to the permeability [36].

ii) CPEI – time (Figure 3b): The effect of CPEI clearly changes depending on the reaction extent. At low reaction time, high CPEI lead to lower permeability levels. On the contrary, low CPEI and time combination results on higher permeability values. As it can be observed, when the reaction time is higher, there is barely a difference on the permeability values depending on the CPEI. As Zhang *et al.* observed, at low reaction

307 times all positions on the membrane surface are suitable of being occupied and PEI
308 molecules could get to the membrane surface with no apparent effort. Nonetheless, at
309 longer reaction times, PEI molecules would be influenced by electrostatic repulsion and
310 steric hindrance and making its way to the surface more difficult [36].

311 Consequently, independently of having higher concentrations of PEI in the solution the
312 thickness of the modification layer will not be increased at long reactions times
313 obtaining similar permeability values.

314 iii) Temperature – time (Figure 3c): As it can be noticed in Figure 3c, the effect of
315 the temperature varies along the reaction time. At minor time, there exists a
316 considerable difference of the effect between high and low temperature effect. The
317 smaller the temperature and the reaction time are, the higher the permeability is.
318 Nonetheless, at long reaction times, the difference of the effect due to the temperature
319 decreases. This situation may occur due to the fact that when time or temperature levels
320 are extensive enough, they permit that an enough amount of PEI molecules would be
321 attached to the membranes. This would become in a thicker modification layer than the
322 one obtained with mild conditions. [36,39,44].

323 For better understanding and corroboration of the presented hypotheses, membrane
324 surface characterization was conducted. Initially, to determine if the modification could
325 have affected the superficial pore size of the membranes, membrane surface SEM
326 micrographs were acquired (Figure 4).
327

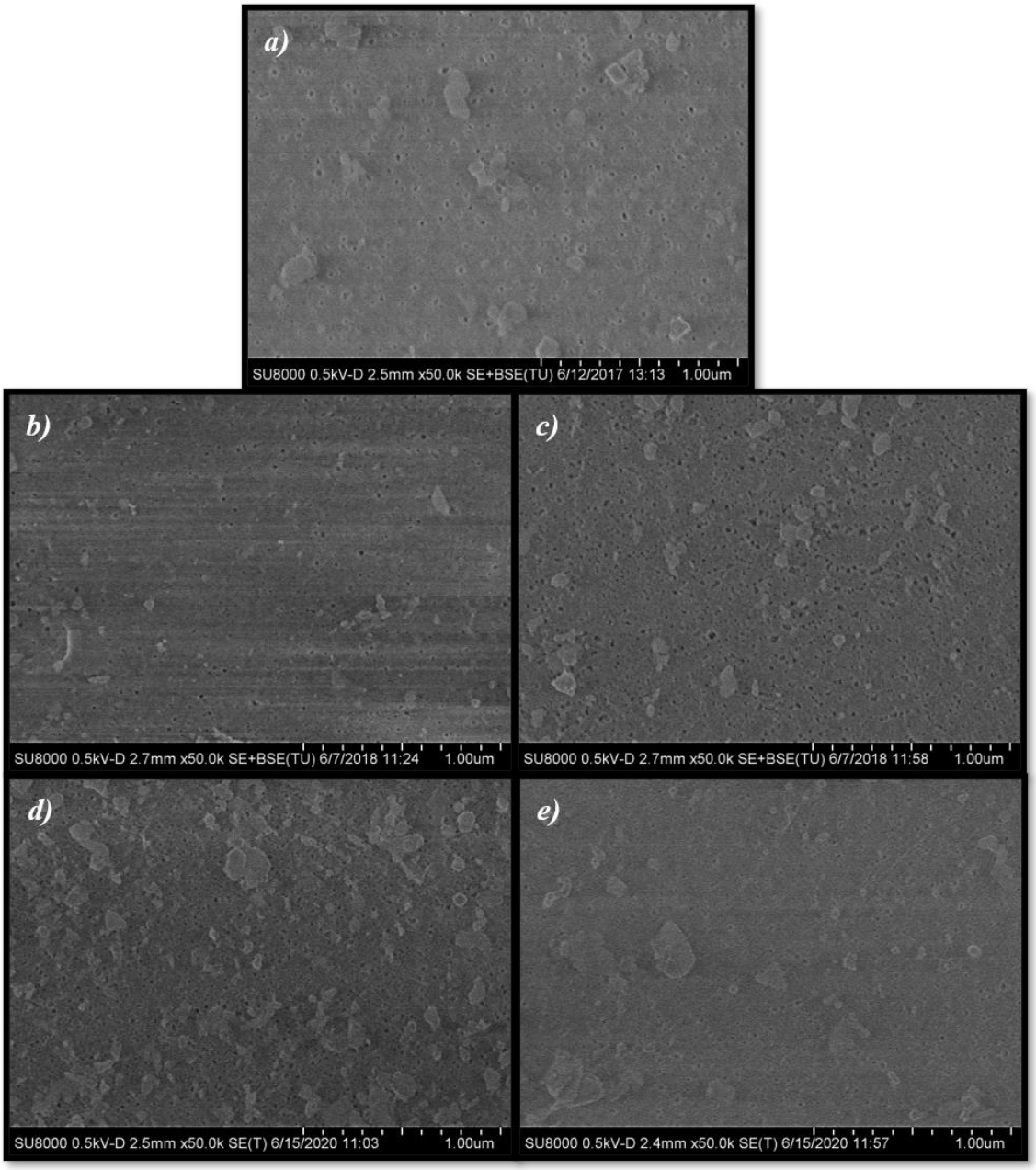

Figure 4 Surface SEM images of a) blank membrane (recycled; no modified), b) Membrane 1 (2h; 30ºC; 1 g/l), c) Membrane 5 (2h; 50ºC; 1 g/l), d) Membrane 9 (7h; 30ºC; 1 g/l) and e) Membrane 13 (7h; 50ºC; 1 g/l)

.

SEM images on Figure 4, showed a very similar surface morphology. Pores can be still perceived in all of them. The estimation of the average pore size, was conducted by DIA following the analytical procedure described in Molina *et al*. [45]. The average pore size, Feret Diameter (d_F), of each membrane was calculated and shown in Table 4.

Table IV Pore diameter values for analyzed membranes

	Feret Diameter, d_F, (nm)
Blank	11.9±6.5
Nº 1	11.3±5.8
Nº 5	11.0±5.3
Nº 9	10.4±5.7
Nº 13	9.8±5.9

As it can be seen in Table 4, pore size presented a minor variation for the different modifications studied. This might be due to the mild conditions used during the modification process. However, it needs to be considered that other studies have shown that when the levels of the modification change (i.e. higher PEI concentration) pore size of the membranes would be affected. [36]. Moreover, membrane surface was examined by the ATR-FTIR spectroscopy. Figure 5 shows ATR-FTIR spectra for the blank and for the selected modified membranes.

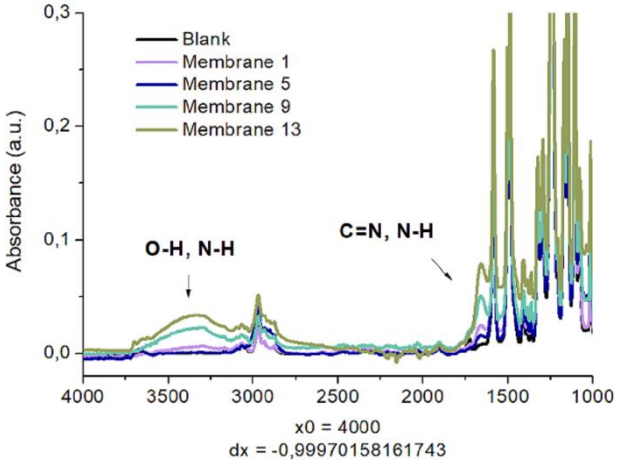

Figure 5 ATR-FTIR spectra

All the spectra were normalized to band at 1240 cm^{-1}, of phenylene ether stretching vibration of the PSF support layer. Spectra from the modified membranes show peaks at 3400 and 1542 cm^{-1} both compatible with amine and alcohol groups, which indicates the co-deposition of the CA and PEI. All studied membranes provided a higher signal than the blank membrane. However, all the obtained signals were considerably weak. This may be due to the mild modification conditions of the selected membranes, which were intentionally chosen to improve membrane characteristics without compromising membrane performance in terms of permeability. The intensity of these signals is especially weak in membranes 1 and 5 (2 hours modification). Even though the parameters on the modification process were varied (30ºC and 50ºC respectively), both membranes showed very similar spectra. Conversely, in the case of membranes 9 and 13 (7 hours modification; 30ºC and 50ºC respectively), although spectra of both membranes still presented a weak signal, the difference between these membranes is more accentuated. This could be explained having into consideration the effect of the interaction between factors. Temperature may lead to a more disorganized reaction which, in combination with low reaction times, could lead to a lower attachment of PEI molecules to the membrane surface. Still, that did not happen at long reaction times resulting on a thicker modification layer for the membrane modified at the highest temperature.

Once more, the intensity of these bands was weak because of the mild conditions set for the surface modification. Consequently, it might happen that the thickness of the deposited layer might be thinner than the penetration depth of ATR beam. For this reason, deeper analysis by mean of XPS was conducted. Table 5 shows the surface element composition of several membranes.

Table V Surface element composition obtained by XPS

	Blank	Membrane 1	Membrane 5	Membrane 9
Carbon %	70.85	64.01	73.59	69.04
Oxygen %	23.73	29.72	19.94	23.63
Nitrogen %	2.65	4.47	3.41	5.40
Sulphur %	2.77	1.79	3.05	1.93
RATIO NITROGEN / SULPHUR				
	0.96	2.49	1.12	2.80

It was detected that the modified membranes have higher atomic percentage of nitrogen than the blank membrane, which could be attributed to the nitrogen element of PEI. Moreover, the N/S ratio of the modified membranes is also superior to the blank. Results of membrane 5 (1:1; 50ºC; 2h), which N/S ratio was lower than membrane 1(1:1; 30ºC; 2h) should be highlighted. These results were in concordance with the ones obtained with FTIR-ATR analysis. As Zhang *et al*. previously reported, due to the endothermic character of the reaction, an increase of the temperature would lead to a higher degree reaction. This would permit more PEI molecules to attach to the membrane surface shortly. [36]. However, it could be possible that this fast PEI attachment also entails an increase of electrostatic repulsion making more difficult for new molecules to reach the surface (Figure 6).

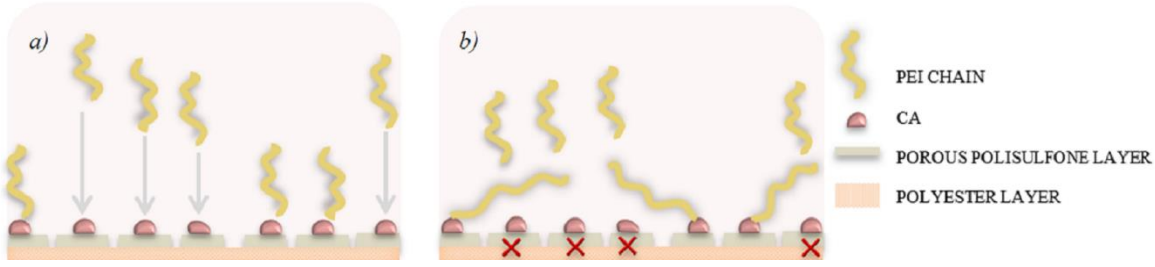

Figure 6 CA-PEI co-deposition reaction scheme: a) Ordered co-deposition reaction; b) Disordered co-deposition reaction.

According to the obtained model, at low reaction time and for low CPEI values, temperature has a negative effect on the attachment of PEI molecules. Moreover,

membrane 1 and 9, both modified at 30º C, presented a very similar N/S ratio even though reaction time is different (2 hours and 7 hours respectively). The reason was that, at the beginning of the reaction, as PEI molecules reach the surface of the membrane very easily. Still, as long as the reaction goes by, PEI molecules have to deal with steric hindrance and a progressive lack of reactive sites for PEI causing a more difficult approaching more and making the reaction grade slower[36].

3.3. Effects of factors and interaction on FRR

Earliest results obtained by running the model showed that FRR values varied from 0% to 50%. Main factors and interactions affecting the *FRR* values are shown in Figure 7 It can be observed that main factors affecting the response are temperature and time both of them negatively

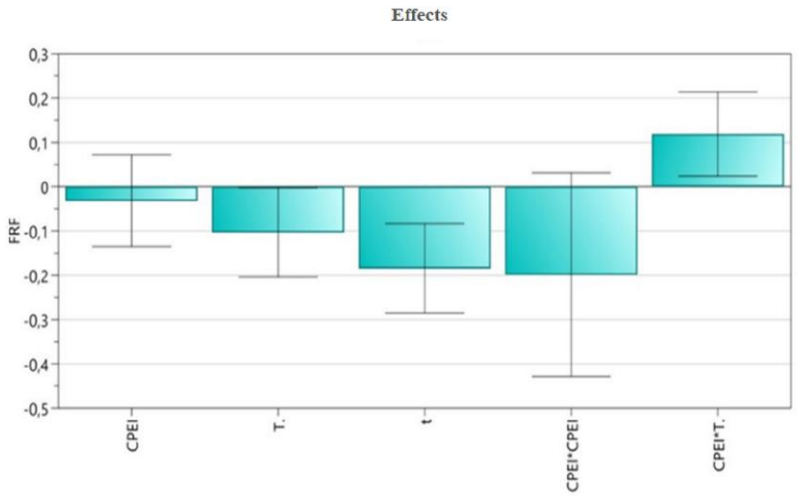

Figure 7. Factors and interaction affecting FRR response. 95% confident level is shown as error bar.

One interaction was statistically significant: CPEI – Temperature (Figure 8).

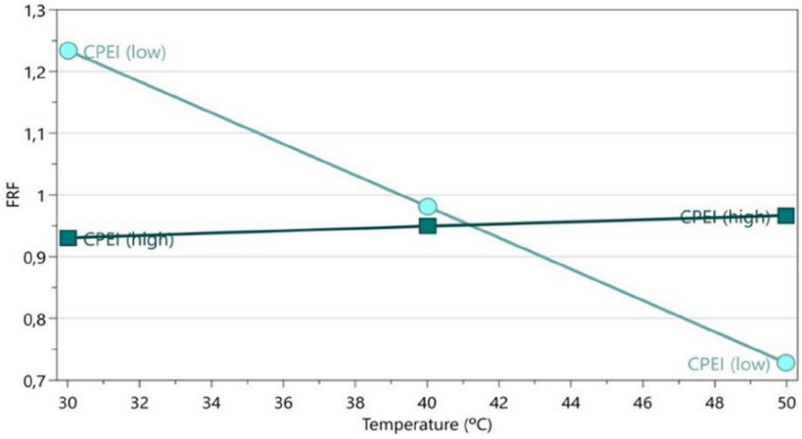

Figure 8 CPEI – Temperature interaction on FRR

The negative effect of time and temperature reaction might be explained because membrane surface roughness was increased. As it can be observed in Figure 8, at high CPEI values, FRR values were rather similar and did not change when increasing the temperature. On the other hand, at low CPEI levels, the FRR values changed significantly with the temperature. At low CPEI and low temperature the reaction was conducted at mild conditions where PEI molecules could reach the reactive sites on membrane surface in a homogeneous way. However, when temperature is high and due to the endothermic character of the reaction, reaction grade will be higher making more PEI molecules reach the surface faster. Due to the deposition, there would be more electrostatic repulsion and steric hindrance, being more difficult for the following PEI molecules to reach the surface homogeneously. Therefore, roughness will be higher. As it was reported in previous works [46,47], membranes with higher roughness tend to have more fouling issues. That is why, membranes with lower roughness would have better FRR.

The effect of main affecting factors and interaction has been analyzed and corroborated together with AFM. Membranes chosen to be evaluated by this technique were those with concentrations of modification solution of 1 g/l modified at different times and temperatures.

Figure 9 shows the AFM images and Table 6 shows the average roughness (R_a, the average deviation of the peaks and valleys regarding the average height) and root mean square roughness (R_q, standard deviation of both valleys and peaks).

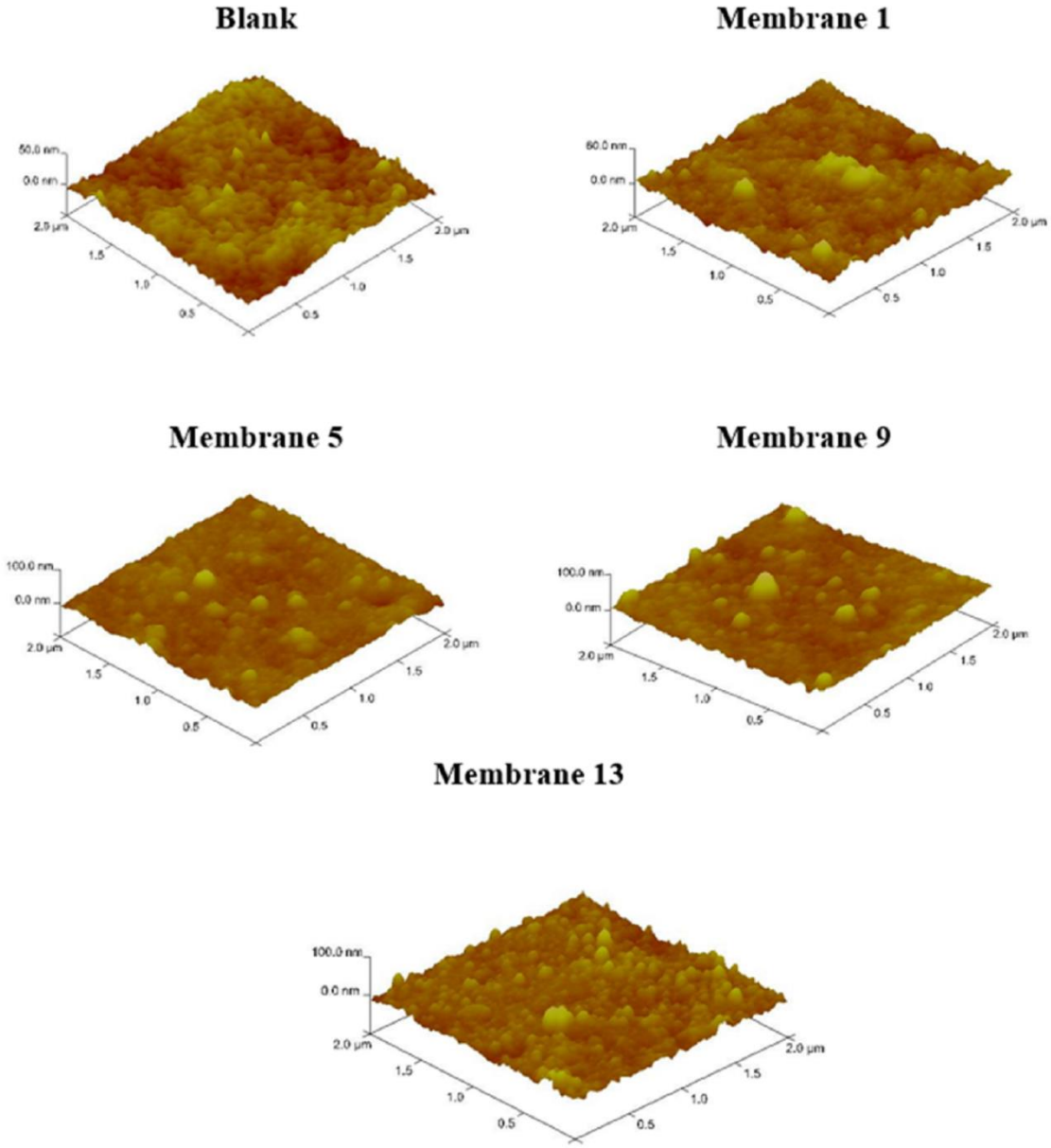

Figure 9 AFM images of the recycled and modified membranes

Table VI Surface roughness of membranes studied by AFM

Membrane	R_a (nm)	R_q(nm)
Blank	4.7±0.6	6.3±1.2
Membrane 1	5.2±0.9	7.5±1.3
Membrane 5	5.7±0.8	7.9±1.3
Membrane 9	8.8±3.0	11.5±4.1
Membrane 13	10.2±2.8	13.5±3.6

As it can be seen, R_a and R_q values of all modified studied membranes are higher than the blank one. It can be observed that at longer reactions time, roughness is higher. Membranes 1 and 5 presented a rather higher roughness values than the blank, although they are not so accentuated. On the other hand, membranes 9 and 13 had a clear intensification on roughness values, compared with membranes 1 and 5. However, in both cases, membranes modified at the highest temperature (50ºC; membranes 5 and 13) presented a slightly higher roughness value in comparison with the membranes which had been modified at same reaction times but lower temperature (30ºC; membranes 1 and 9). This fact might be explained by taking into consideration the characteristics of the chemical reaction as it was explained in section 3.2. PEI molecules reach the membrane via Michael and/or Schiff endothermic reactions. Faster reaction might cause that all PEI brushes would not reach the surface in an identical or homogeneous position boosting the steric hindrance of the reaction. (Figure 10) [36].

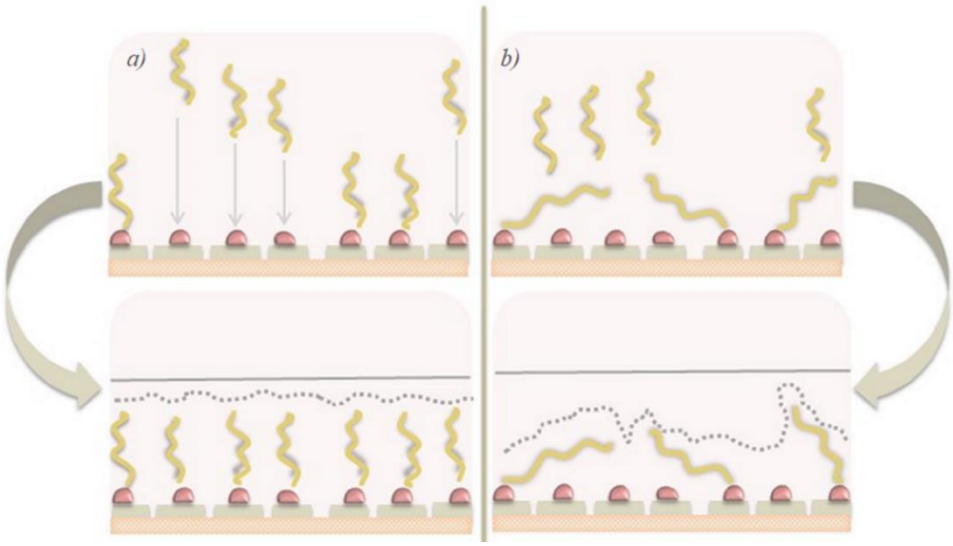

Figure 10 Surface roughness: a) Roughness resultant in an ordered co-deposition reaction; b) Roughness resultant in a disordered co-deposition reaction

It is important to note that although membranes 1 and 9 were modified with the same temperature (30ºC), membrane 9 showed superior roughness than membrane 1. During the time the co-deposition reaction is happening more molecules of PEI would be able

to reach a position on membrane surface. Still, the more the PEI molecules are, the more the electrostatic repulsion forces are and the less the free spaces to attached are. This situation would lead to more PEI molecules trying to reach the surface in a more disorganized form. Consequently, the surface roughness would be increased with both, time and temperature.

4. Conclusions and future work

In this study surface modification by dip-coating of recycled membrane with environmentally friendly compounds (CA and PEI) was successfully conducted, obtaining improvements on the membrane performance. Statistical design of experiments demonstrated to be a very valuable tool to develop the study of membrane surface modification using CA and PEI and its performance. Membranes with higher roughness presented a worst flux recovery after fouling experiments. In addition, long reaction times used in the dip coating process resulted in thicker modification layer.

Given the results obtained when the model was fitted, it was demonstrated that the interactions between factors were as much significant as the main factors. Considering the improvement of R_p and FRR, having surface modification at mild conditions (1 g/l CA: 1 g/l PEI 600 Mw; 30 ºC; 2 hours) seem to obtain best membrane process performance for our study (R_p = 1.12; FRR = 1.38). In addition, conducting surface modification in mild conditions follows the path of working at low energy and chemicals consumption. This combined with the use of recycled membranes could be a very interesting alternative for those processes that have a high membrane replacement rate and/or important fouling issues such as membrane bioreactors (MBR). Following this approach, further studies will be conducted where recycled and modified UF membranes will be used in MBRs for urban wastewater treatment. In addition, further optimization experiments using statistical design of experiments should be conducted in

order to optimize the surface modification process. Finally, this study shows that the combination of recycled membranes modified with bio inspired low-cost surface modification along with the obtained results is very promising in terms of sustainability in membrane technology.

Acknowledgements

This research is part of the national projects: INREMEM (Innovation and recycling of membranes for water treatment, Ref. CTM2015-65348-C2-1-R; (MINECO/FEDER, UE)) and INREMEM 2.0 (Hybrid wastewater treatments based on recycled membranes with the objective of zero liquid discharge (ZLD), Ref. RTI2018-096042-B-C21 (MCIU/AEI/FEDER, UE)), and they are supported by the Spanish Ministry of Science and Innovation and co-financed by the European Regional Development Fund (ERDF) and the Spanish State Research Agency (AEI).

References

[1] S. Alzahrani, A.W. Mohammad, Challenges and trends in membrane technology implementation for produced water treatment: A review, J. Water Process Eng. 4 (2014) 107–133. https://doi.org/10.1016/j.jwpe.2014.09.007.

[2] A. Yusuf, A. Sodiq, A. Giwa, J. Eke, O. Pikuda, G. De Luca, J.L. Di Salvo, S. Chakraborty, A review of emerging trends in membrane science and technology for sustainable water treatment, J. Clean. Prod. 266 (2020) 121867. https://doi.org/10.1016/j.jclepro.2020.121867.

[3] K.P. Lee, T.C. Arnot, D. Mattia, A review of reverse osmosis membrane materials for desalination-Development to date and future potential, J. Memb. Sci. 370 (2011) 1–22. https://doi.org/10.1016/j.memsci.2010.12.036.

[4] A. Suárez, P. Fernández, J. Ramón Iglesias, E. Iglesias, F.A. Riera, Cost assessment of membrane processes: A practical example in the dairy wastewater reclamation by reverse osmosis, J. Memb. Sci. 493 (2015) 389–402. https://doi.org/10.1016/j.memsci.2015.04.065.

[5] A. Ruiz-García, E. Ruiz-Saavedra, 80,000h operational experience and performance analysis of a brackish water reverse osmosis desalination plant. Assessment of membrane replacement cost, Desalination. 375 (2015) 81–88. https://doi.org/10.1016/j.desal.2015.07.022.

[6] R. García-Pacheco, J. Landaburu-Aguirre, S. Molina, L. Rodríguez-Sáez, S.B. Teli, E. García-Calvo, Transformation of end-of-life RO membranes into NF and UF membranes: Evaluation of membrane performance, J. Memb. Sci. 495 (2015). https://doi.org/10.1016/j.memsci.2015.08.025.

[7] A European Strategy for Plastics in a Circular Economy. Brussels Title, COM 28 Final. (2018). https://eur-lex.europa.eu/.

[8] European Comission, https://ec.europa.eu/environment/circular-economy/, (n.d.) https://ec.europa.eu/environment/circular-economy/.

[9] W. Lawler, Z. Bradford-Hartke, M.J. Cran, M. Duke, G. Leslie, B.P. Ladewig, P. Le-Clech, Towards new opportunities for reuse, recycling and disposal of used reverse osmosis membranes, Desalination. 299 (2012) 103–112. https://doi.org/10.1016/j.desal.2012.05.030.

[10] J. Landaburu-Aguirre, R. García-Pacheco, S. Molina, L. Rodríguez-Sáez, J. Rabadán, E. García-Calvo, Fouling prevention, preparing for re-use and membrane recycling. Towards circular economy in RO desalination, Desalination. 393 (2016) 16–30. https://doi.org/10.1016/j.desal.2016.04.002.

[11] W. Lawler, J. Alvarez-Gaitan, G. Leslie, P. Le-Clech, Comparative life cycle assessment of end-of-life options for reverse osmosis membranes, Desalination. 357 (2015) 45–54. https://doi.org/10.1016/j.desal.2014.10.013.

[12] W. Lawler, A. Antony, M. Cran, M. Duke, G. Leslie, P. Le-Clech, Production and characterisation of UF membranes by chemical conversion of used RO membranes, J. Memb. Sci. 447 (2013) 203–211. https://doi.org/10.1016/j.memsci.2013.07.015.

[13] J. de A. S. Molina, R. García-Pacheco, L. Rodríguez-Sáez, E. García-Calvo, E. Campos, D. Zarzo, J.G. de la Campa, Transformation of end-of-life RO membranes into recycled NF and UF membranes, surface characterization, in: IDA World Congr., San Diego, California, 2015.

[14] J.J. Rodríguez, V. Jiménez, O. Trujillo, J. Veza, Reuse of reverse osmosis membranes in advanced wastewater treatment, Desalination. 150 (2002) 219–225. https://doi.org/10.1016/S0011-9164(02)00977-3.

[15] J.M. Veza, J.J. Rodriguez-Gonzalez, Second use for old reverse osmosis

membranes: Wastewater treatment, Desalination. 157 (2003) 65–72. https://doi.org/10.1016/S0011-9164(03)00384-9.
[16] R. García-Pacheco, J. Landaburu-Aguirre, P. Terrero-Rodríguez, E. Campos, F. Molina-Serrano, J. Rabadán, D. Zarzo, E. García-Calvo, Validation of recycled membranes for treating brackish water at pilot scale, Desalination. 433 (2018) 199–208. https://doi.org/10.1016/j.desal.2017.12.034.
[17] R.H. Hailemariam, Y.C. Woo, M.M. Damtie, B.C. Kim, K.D. Park, J.S. Choi, Reverse osmosis membrane fabrication and modification technologies and future trends: A review, Adv. Colloid Interface Sci. 276 (2020) 102100. https://doi.org/10.1016/j.cis.2019.102100.
[18] K. Xiao, S. Liang, X. Wang, C. Chen, X. Huang, Current state and challenges of full-scale membrane bioreactor applications: A critical review, Bioresour. Technol. 271 (2019) 473–481. https://doi.org/10.1016/j.biortech.2018.09.061.
[19] A.G. Fane, A grand challenge for membrane desalination: More water, less carbon, Desalination. 426 (2018) 155–163. https://doi.org/10.1016/j.desal.2017.11.002.
[20] J. Senán-Salinas, R. García-Pacheco, J. Landaburu-Aguirre, E. García-Calvo, Recycling of end-of-life reverse osmosis membranes: Comparative LCA and cost-effectiveness analysis at pilot scale, Resour. Conserv. Recycl. 150 (2019) 104423. https://doi.org/10.1016/j.resconrec.2019.104423.
[21] Z. Zhang, M.W. Bligh, Y. Wang, G.L. Leslie, H. Bustamante, T.D. Waite, Cleaning strategies for iron-fouled membranes from submerged membrane bioreactor treatment of wastewaters, J. Memb. Sci. 475 (2015) 9–21. https://doi.org/10.1016/j.memsci.2014.09.003.
[22] W. Zhang, F. Jiang, Membrane fouling in aerobic granular sludge (AGS)-membrane bioreactor (MBR): Effect of AGS size, Water Res. 157 (2019) 445–453. https://doi.org/10.1016/j.watres.2018.07.069.
[23] W. Zhang, W. Liang, Z. Zhang, T. Hao, Aerobic granular sludge (AGS) scouring to mitigate membrane fouling: Performance, hydrodynamic mechanism and contribution quantification model, Water Res. 188 (2021) 116518. https://doi.org/10.1016/j.watres.2020.116518.
[24] H. Sun, Y. Chen, J. Liu, D. Chai, P. Li, M. Wang, Y. Hou, Q. Jason Niu, A novel chlorine-resistant polyacrylate nanofiltration membrane constructed from oligomeric phenolic resin, Sep. Purif. Technol. 262 (2021) 118300. https://doi.org/10.1016/j.seppur.2021.118300.
[25] R.A. Lusiana, V.D.A. Sangkota, N.A. Sasongko, G. Gunawan, A.R. Wijaya, S.J. Santosa, D. Siswanta, M. Mudasir, M.N.Z. Abidin, S. Mansur, M.H.D. Othman, Permeability improvement of polyethersulfone-polietylene glycol (PEG-PES) flat sheet type membranes by tripolyphosphate-crosslinked chitosan (TPP-CS) coating, Int. J. Biol. Macromol. 152 (2020) 633–644. https://doi.org/10.1016/j.ijbiomac.2020.02.290.
[26] H. Lee, K.D. Lee, K.B. Pyo, S.Y. Park, H. Lee, Catechol-grafted poly(ethylene glycol) for PEGylation on versatile substrates, Langmuir. 26 (2010) 3790–3793. https://doi.org/10.1021/la904909h.
[27] W. Chen, J. Mo, X. Du, Z. Zhang, W. Zhang, Biomimetic dynamic membrane for aquatic dye removal, Water Res. 151 (2019) 243–251. https://doi.org/10.1016/j.watres.2018.11.078.
[28] P.S. Goh, A.K. Zulhairun, A.F. Ismail, N. Hilal, Contemporary antibiofouling modifications of reverse osmosis desalination membrane: A review, Desalination. 468 (2019). https://doi.org/10.1016/j.desal.2019.114072.
[29] L. Upadhyaya, X. Qian, S. Ranil Wickramasinghe, Chemical modification of membrane surface — overview, Curr. Opin. Chem. Eng. 20 (2018) 13–18. https://doi.org/10.1016/j.coche.2018.01.002.

[30] S.A. Deowan, F. Galiano, J. Hoinkis, D. Johnson, S.A. Altinkaya, B. Gabriele, N. Hilal, E. Drioli, A. Figoli, Novel low-fouling membrane bioreactor (MBR) for industrial wastewater treatment, J. Memb. Sci. 510 (2016) 524–532. https://doi.org/10.1016/j.memsci.2016.03.002.
[31] J. Ayyavoo, T.P.N. Nguyen, B.M. Jun, I.C. Kim, Y.N. Kwon, Protection of polymeric membranes with antifouling surfacing via surface modifications, Colloids Surfaces A Physicochem. Eng. Asp. 506 (2016) 190–201. https://doi.org/10.1016/j.colsurfa.2016.06.026.
[32] N. Nady, M.C.R. Franssen, H. Zuilhof, M.S.M. Eldin, R. Boom, K. Schroën, Modification methods for poly(arylsulfone) membranes: A mini-review focusing on surface modification, Desalination. 275 (2011) 1–9. https://doi.org/10.1016/j.desal.2011.03.010.
[33] J. Ayyavoo, T.P.N. Nguyen, B.M. Jun, I.C. Kim, Y.N. Kwon, Protection of polymeric membranes with antifouling surfacing via surface modifications, Colloids Surfaces A Physicochem. Eng. Asp. 506 (2016) 190–201. https://doi.org/10.1016/j.colsurfa.2016.06.026.
[34] H. Saleem, S.J. Zaidi, Nanoparticles in reverse osmosis membranes for desalination: A state of the art review, Desalination. 475 (2020) 114171. https://doi.org/10.1016/j.desal.2019.114171.
[35] N.Z. Department of Chemical and Materials Engineering, The University of Auckland, Private Bag 92019, Auckland, Control of Polyaniline Deposition on Microporous Cellulose Ester Membranes by in Situ Chemical Polymerization, J. Phys. Chem. 113, 45 (2009) 14986–14993. https://doi.org/10.1021/jp9038336.
[36] R. Zhang, Y. Su, X. Zhao, Y. Li, J. Zhao, Z. Jiang, A novel positively charged composite nanofiltration membrane prepared by bio-inspired adhesion of polydopamine and surface grafting of poly(ethylene imine), J. Memb. Sci. 470 (2014) 9–17. https://doi.org/10.1016/j.memsci.2014.07.006.
[37] B.D. McCloskey, H.B. Park, H. Ju, B.W. Rowe, D.J. Miller, B.D. Freeman, A bioinspired fouling-resistant surface modification for water purification membranes, J. Memb. Sci. 413–414 (2012) 82–90. https://doi.org/10.1016/j.memsci.2012.04.021.
[38] C. Cheng, S. Li, W. Zhao, Q. Wei, S. Nie, S. Sun, C. Zhao, The hydrodynamic permeability and surface property of polyethersulfone ultrafiltration membranes with mussel-inspired polydopamine coatings, J. Memb. Sci. 417–418 (2012) 228–236. https://doi.org/10.1016/j.memsci.2012.06.045.
[39] Y.C. Xu, Z.X. Wang, X.Q. Cheng, Y.C. Xiao, L. Shao, Positively charged nanofiltration membranes via economically mussel-substance-simulated co-deposition for textile wastewater treatment, Chem. Eng. J. 303 (2016) 555–564. https://doi.org/10.1016/j.cej.2016.06.024.
[40] S. Xue, C. Li, J. Li, H. Zhu, Y. Guo, A catechol-based biomimetic strategy combined with surface mineralization to enhance hydrophilicity and anti-fouling property of PTFE flat membrane, J. Memb. Sci. 524 (2017) 409–418. https://doi.org/10.1016/j.memsci.2016.11.075.
[41] W.Z. Qiu, Z.S. Zhao, Y. Du, M.X. Hu, Z.K. Xu, Antimicrobial membrane surfaces via efficient polyethyleneimine immobilization and cationization, Appl. Surf. Sci. 426 (2017) 972–979. https://doi.org/Get rights and content.
[42] J. Landaburu-Aguirre, E. Pongrácz, P. Perämäki, R.L. Keiski, Micellar-enhanced ultrafiltration for the removal of cadmium and zinc: Use of response surface methodology to improve understanding of process performance and optimisation, J. Hazard. Mater. 180 (2010) 524–534. https://doi.org/10.1016/j.jhazmat.2010.04.066.
[43] W.S. Rasband, ImageJ, U. S. National Institutes of Health, Bethesda, Maryland,

USA, 1997-2014, http://imagej.nih.gov/ij/., (n.d.).
[44] F. Zarei, R.M. Moattari, S. Rajabzadeh, M. Bagheri, A. Taghizadeh, T. Mohammadi, H. Matsuyama, Preparation of thin film composite nano-filtration membranes for brackish water softening based on the reaction between functionalized UF membranes and polyethyleneimine, J. Memb. Sci. 588 (2019) 117207. https://doi.org/10.1016/j.memsci.2019.117207.
[45] S. Molina, P. Carretero, S.B. Teli, J.G. De la Campa, Á.E. Lozano, J. De Abajo, Hydrophilic porous asymmetric ultrafiltration membranes of aramid-g-PEO copolymers, J. Memb. Sci. 454 (2014) 233–242. https://doi.org/10.1016/j.memsci.2013.11.025.
[46] S.H. Woo, B.R. Min, J.S. Lee, Change of surface morphology, permeate flux, surface roughness and water contact angle for membranes with similar physicochemical characteristics (except surface roughness) during microfiltration, Sep. Purif. Technol. 187 (2017) 274–284. https://doi.org/10.1016/j.seppur.2017.06.030.
[47] Z. Zhong, D. Li, B. Zhang, W. Xing, Membrane surface roughness characterization and its influence on ultrafine particle adhesion, Sep. Purif. Technol. 90 (2012) 140–146. https://doi.org/10.1016/j.seppur.2011.09.016.

Abbreviations

AFM

Atomic force microscopy

ANOVA

Analysis of variance

ATR–FTIR

Attenuated total reflectance–Fourier transform infrared spectroscopy

BSA

Bovine Serum Albumin

CA

Catechol

DIA

Digital Image Analysis

EoL

End-of-life

FRR

Flux recovery ratio

LCA

Life Cycle Assessment

MLR

Multiple linear regressions

NaClO

Sodium hypochlorite

PA

Polyamide

PDA

Polydopamine

PEI

Polyetylenimine

Pr

Relative permeability

RO

Reverse osmosis

SEM

Scanning electron microscopy

UF

Ultrafiltration

XPS

X-ray photoelectron spectroscopy

Nomenclature

ρ

Solution density (g/L)

A

Membrane effective area (m^2)

*C*CA

Catechol concentration (g/L)

717 *C*PEI

718 Polyethileneimine concentration (g/L)

719 DF

720 Degrees of freedom

721 $F_{tabulated}$

722 Fisher test critical value

723 *F* value

724 Fisher test calculated value

725 *h*

726 Time (hours)

727 *J*

728 Permeate flux ($L \cdot m^{-2} \cdot h^{-1}$)

729 MS

730 Mean square

731 *P*

732 Permeability ($L \cdot m^{-2} \cdot h^{-1} \cdot bar^{-1}$)

733 $P_{average}$

734 Average permeability ($L \cdot m^{-2} \cdot h^{-1} \cdot bar^{-1}$)

735 P_i

736 Individual permeability ($L \cdot m^{-2} \cdot h^{-1} \cdot bar^{-1}$)

737 P_r

738 Relative permeability ($L \cdot m^{-2} \cdot h^{-1} \cdot bar^{-1}$)

739 *p*-value

740 Probability

741 PRESS

742 Prediction residual sum of squares

743 Q

744 Membranes permeate flow ($L.h^{-1}$)

745 Q^2

746 Response variation percentage predicted by the model

747 R^2

748 Coefficient of determination

749 R^2_{adj}

750 Adjusted coefficient of determination

751 S

752 Membrane surface (m^2)

753 SD

754 Standard deviation

755 SS

756 Sum of squares

757 t

758 Time (hours)

759 T

760 Temperature (ºC)

761 TMP

762 Transmembrane pressure (bar)

763 W

764 Permeate weight (g)

765

Images captions

Figure 1

Membrane preparation flow chart

Figure 2

Effects on relative permeability (MODDE_12 Software). 95% confident level is shown as error bar

Figure 3

Interactions affecting relative permeability: a) CPEI - Temperature; b) CPEI – Time; c) Temperature – Time

Figure 4

Surface SEM images of a) blank membrane (recycled; no modified), b) Membrane 1 (2h; 30ºC; 1 g/l), c) Membrane 5 (2h; 50ºC; 1 g/l), d) Membrane 9 (7h; 30ºC; 1 g/l) and e) Membrane 13 (7h; 50ºC; 1 g/l)

Figure 5

ATR-FTIR spectra

Figure 6

CA-PEI co-deposition reaction scheme: a) Ordered co-deposition reaction; b) Disordered co-deposition reaction

Figure 7

Factors and interaction affecting FRR response. 95% confident level is shown as error bar

Figure 8

CPEI – Temperature interaction on FRR

Figure 9

AFM images of the recycled and modified membranes

Figure 10

Surface roughness: a) Roughness resultant in an ordered co-deposition reaction; b) Roughness resultant in a disordered co-deposition reaction